JOURNAL OF OPTOELECTRONICS AND ADVANCED MATERIALS Vol. 12, No. 9, September 2010, p. 1909 - 1914

# Solution-based synthesis of semiconductive oxide 1-D nanostructures

V. MUSAT*, E. FORTUNATO[a], M. MAZILU, T. BUSANI[a], B. DIACONU[a], M. DOBRE
*Centre of Nanostructures and Functional Materials-CNMF, "Dunărea de Jos" University of Galati, 111 Domneasca, 800201, Galati, Romania*
[a]*Departamento de Ciência dos Materiais-CENIMAT/I3N, New University of Lisbon, Portugal*

One-dimensional semiconductive oxide nanomaterials such as nanowires or nanorods have focused much attention due to their multifunctionality in the field of nanoelectronics and photoelectronics, photocatalysis, gas sensing, piezoelectricity or thin film transistors for transparent and flexible electronics. Transition-metals doped zinc oxide is generating much interest also for the novel magnetic properties so called "dilute magnetic semiconductors" and are envisioned to be potential building blocks for spintronic devices. Solution-phase chemical synthesis of the nanomaterials have several important advantages, as high versatility, low cost, simple equipments and handling, in additon to the ecological benefits. *Chemical bath deposition* (CBD) methods is one of the most used methods for growing crystallized oxides nanostructures from aqueous solution at temperatures below 100°C. In this paper we present some results on the CBD synthesis and characterization of ZnO-based 1D nanostructures.

(Received August 2, 2010; accepted September 15, 2010)

*Keywords:* Chemical bath deposition, 1D nanoparticles, Zinc oxide, Morphology, Crystalline structure, Electrical properties

## 1. Introduction

One-dimentional nanostructures of semiconductor materials are currently of considerable interest due to their importance in scientific research and great potential of applications [1-6]. ZnO is a transition metal oxide that generally crystallizes in the hexagonal structure with lattice parameters a = 3.25 Å and c = 5.20 Å [7]. Due to its wide band gap of 3.37 eV and large exciton binding energy of 60 meV, the nanometer-sized ZnO is one of the most promising materials for optoelectronic application and has a great potential in photocatalysis for the degradation of organic pollutants existing in water and air. Typically, the photoluminescence spectra of ZnO has emission bands in the UV and visible (green, blue, violet) regions [3, 8, 9]. ZnO nanoparticles are also used in surface acoustic wave devices (SAW) [3, 5, 10] and gas sensor devices. Nanoparticles and 1D nanostructued thin films of ZnO have been proposed for CO, $NH_3$, alcohol and $H_2$ sensing under elevated temperature (~400°C) [7, 11, 12, 13]. Devi et al. have reported the sensing properties of nanocrystalline ZnO-based thick films for $NH_3$ and Baruwati et al. (2006) also reported the gas-sensing properties of highly crystallized ZnO nanoparticles (Patra et al. 2008).

Solution-phase chemical synthesis of the nanomaterials have several important advantages, as high versatility, low cost, simple equipments and handling, in additon to the ecological benefits.

In this paper we present some results on the chemical synthesis and characterization of ZnO 1D nanomaterials. Chemical bath deposition method has been used in order to growth ZnO nanorods and nanowires structures on glass substrate seeded with different thin film as gold-nanoparticles [14], ZnO nanoparticle [15-18] and sol-gel derived ZnO thin film [19]. The effect of the morphology and microstructure of the seeding thin film on the morphology, aspect ratio (length divided by width) and crystalline structure of the obtained nanostructures were investigated.

## 2. Experimental

ZnO nanowires were grown on glass substrate using a simple two-step process: substrate seeding with a catalytic thin film of gold nanoparticles or ZnO nanoparticles (step I) followed by ZnO nanostructures growth (step II). In the first step, dip coating method has been used for seeding the glass substrates with gold nanoparticles, pre-prepared ZnO nanoparticles and sol-gel derived ZnO nanoparticles. All the reagents (analytical grade purity) were purchased from Sigma Aldrich. They were used as received without any further purification Colloidal dispersion of ZnO nanoparticles (0.04 M) was obtained by dispersing the ZnO nanoparticles (Sigma Aldrich) with size less than 50 nm in isopropanol in the presence of Polyvinylpyrrolidone (PVP10) in molar ratio ZnO NPs: PVP10 = 1: 0.10 on the ultrasonic bath for 10 min. To prepare Au nanoparticles, 4 mg $HAuCl_4$ were dissolved in 35 ml deionized water by heating to boiling over to add 10 ml aqueous solution of sodium citrate (0.3 mM). After film deposition, the seeded substrates were pre-annealed at 90°C for 10 min and post-annealed at 250°C for 20 min. In the second step, ZnO nanostructures were grown by suspending the seeded substrates in a sealed bottle containing zinc nitrate hydrate

(0.01 M) and hexamethylenetetramine (HMT) aqueous solution, at 90°C. After 2 or 3 h time of reaction, the substrate with grown nanostructures is removed from the solution and dried for 1 h at 90°C.

*The morphology* of the seeded substrates and grown 1-D nanostructures was analyzed by atomic force microscopy (AFM) and scanning electron microscopy (SEM). SEM investigations were made using a Hitachi S-1400 field emission microscope. Tapping mode AFM experiments 114 were performed on a Nanoscope IIIa Multimode AFM microscope 115 (Digital Instruments, Veeco). Commercial etched silicon tips with 116 typical resonance frequency of ca. 300 Hz (RTESP, Veeco) were used 117 as AFM probes.

*The XRD patterns* of the samples were recorded at room temperature using a Rigaku diffractometer (model RAD IIA), with CuKα radiation.

*The FTIR spectra* of ZnO nanostructurs grown on Si substrate was recorded using a UV-VIS-NIR double beam spectrophotometer (UV-3100 PC, Shimadzu) in the wavelength range from 200 to 2500 nm.

*The electrical properties* of the grown nanostructures were measured in dark (special chamber) and vacuum at room temperature and variable temperature using PVD-deposed Al electrodes and a Keithley 6517 A electrometer. The study of the dark conductivity was performed in a dedicated system, consisting of a cryostat and electrometer (KEITHLEY model 238) controlled by a computer. The experiment took place within the temperature range between 270 - 423 K with a variation of the applied voltage between -100 V and +100 V; the data was recorded after 120 seconds after temperature stabilization. The samples were pre-treated by annealing for 30 minutes at 423 K.

## 3. Results and discussion

Figs. 1-3 show the 2D and 3D morphology on the surface of substrates seeded with different thin films of gold nanoparticles (Fig. 1), pre-prepared ZnO nanoparticles (Fig. 2) and sol-gel drived ZnO thin film (Fig. 3).

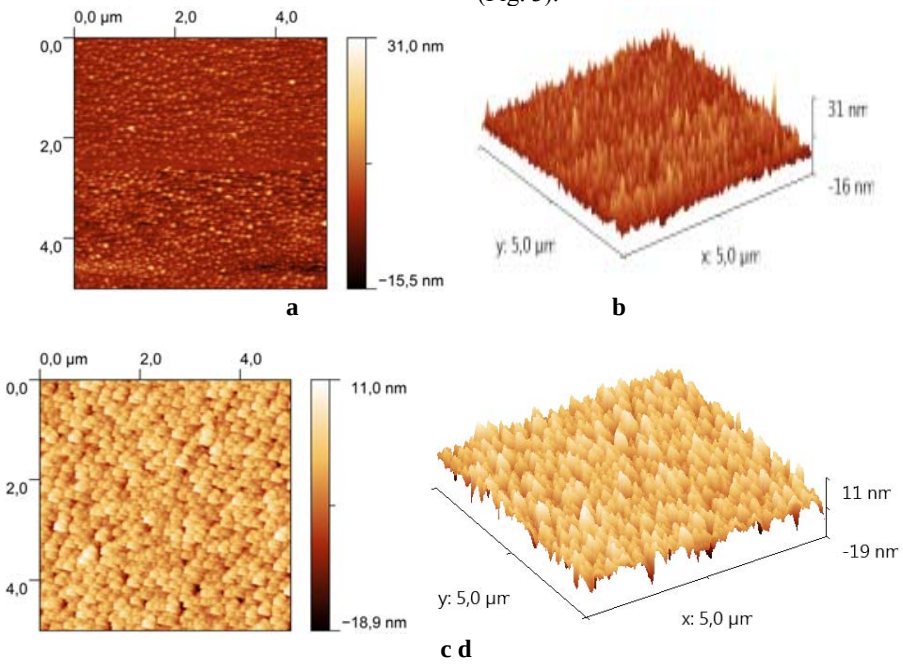


*Fig 1. AFM 2D and 3D morphology of substrates seeded with gold nanoparticles thin films deposed at 1,5 cm/min (a-b) and 10 cm/min (c-d) .*

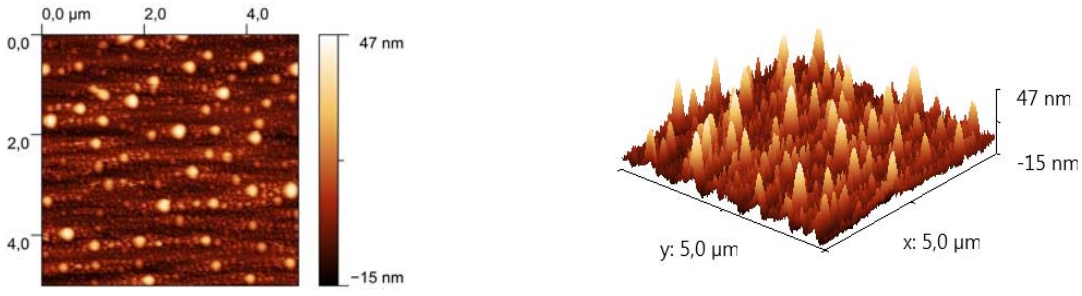


*Fig 2. AFM 2D and 3D morphology of pre-prepared ZnO nanoparticles thin films seeded substrate, at 1.5 cm/min.*

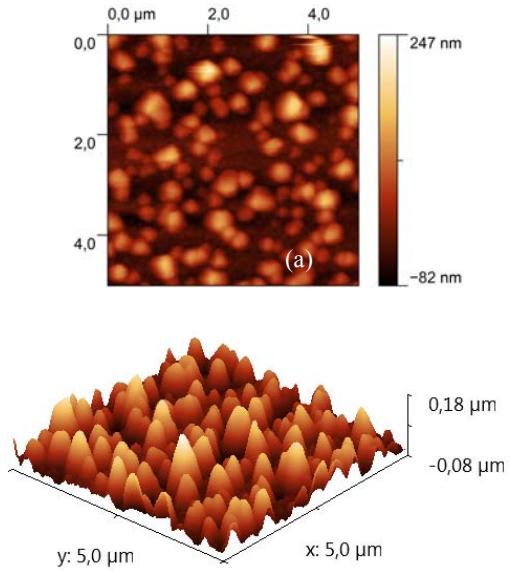


*Fig 3. AFM 2D and 3D morphology of sol-gel drived ZnO thin films seeded substrate at 10 cm/min.*

Fig. 4 shows the X-ray diffraction pattern of ZnO sol-gel drived thin film used as seeds for growing ZnO nanostructures. The XRD pattern confirms that the nanoparticles observed on the seeded substrate (Fig. 3) are wurtzite type ZnO nanocrystals with (002) preferential plane orientation perpendicular to the substrate.

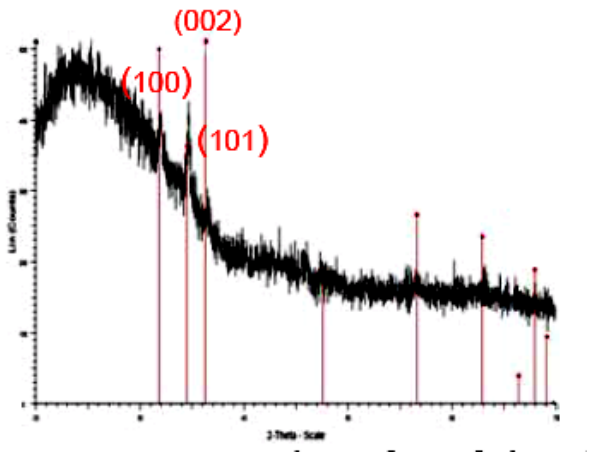


*Fig. 4. XRD patterns on the surface of the sol-gel sedeed substrate, at 5 cm/min.*

The SEM images (Figs. 5 and 6) show the formation of nanorod-like grains morphology structure with general grain orientation perpendicular to the substrate surface. The aspect ratios (length divided by width) of nanorods ranges from 6 to 10. The morphology of the seeded substrate significantly affects the grain orientation and the aspect ratio of 1D nanostrucures.

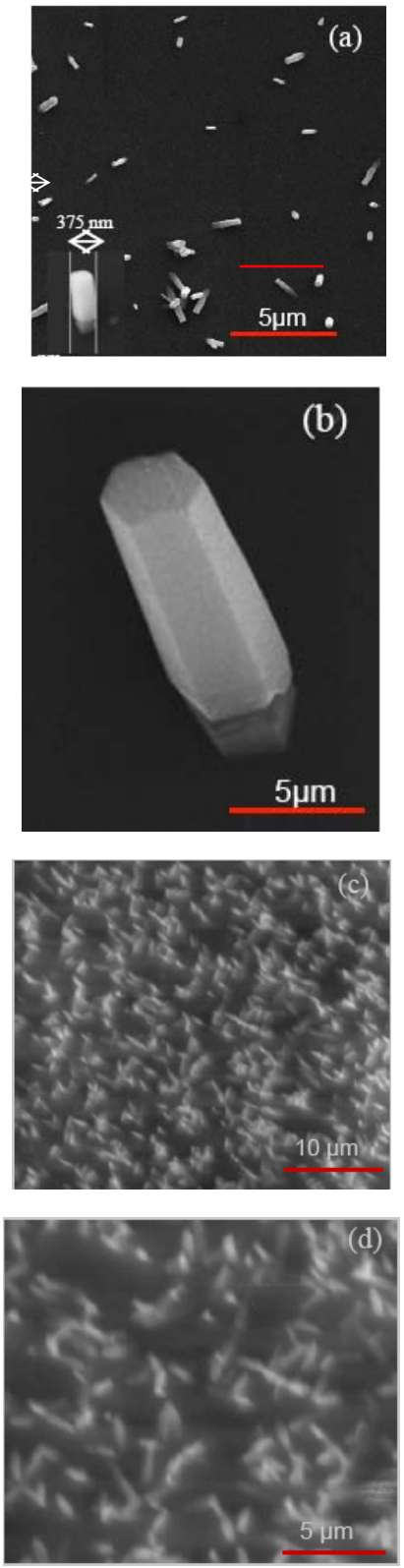


*Fig 5. SEM surface morphology of ZnO 1D nanosctructures grown on substrates seeded with gold nanoparticles thin films deposed at 1,5 cm/min (a-b) and 10 cm/min (c-d).*

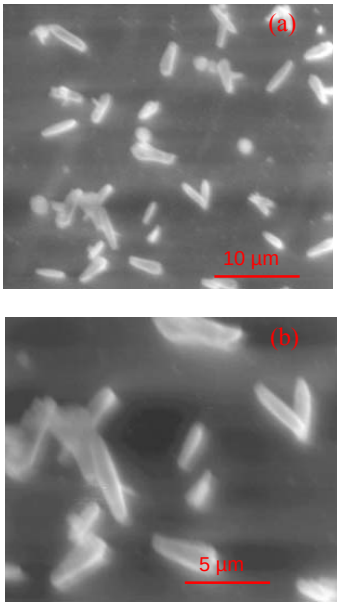


*Fig 6. AFM 2D and 3D morphology of ZnO 1D nanostructures grown on substrate seeded with preprepared ZnO nanoparticles thin films.*

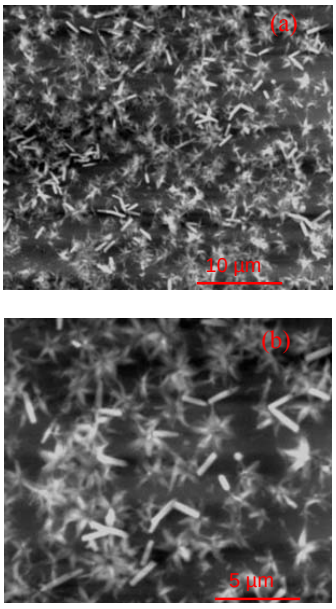


*Fig 7. SEM imagines of ZnO 1D nanomaterials grown on glass substrate seeded with sol-gel-derived ZnO thin film*

Regarding the samples grown on a sol-gel drived thin film, the SEM images (Fig. 7) shows a more complex morphology, both individual nanorod-like and self-assembled flower-like nanostructures are present. This structure is also characterized by a wurtzite type crystal structure but with a different preferred orientation than the other samples. In this case, the preferential crystal orientation is along (100) plan, parallel to the substrate surface, as confirmed by SEM images (Fig. 7).

The X-ray diffraction patterns of the as-grown ZnO nanostructures, which surface morphology is shown the previous figures, are presented in Figure 8. These patterns show, in the 2θ range 30-40, the most important three peaks of hexagonal wurtzite type ZnO structure. In contrast with the normal random orientation of the hexagonal structure of ZnO powder, with (101) most intense peak, these patterns show a (002) dominating peak which indicate a preferential *c*-axis orientation of the nanostructured grains.

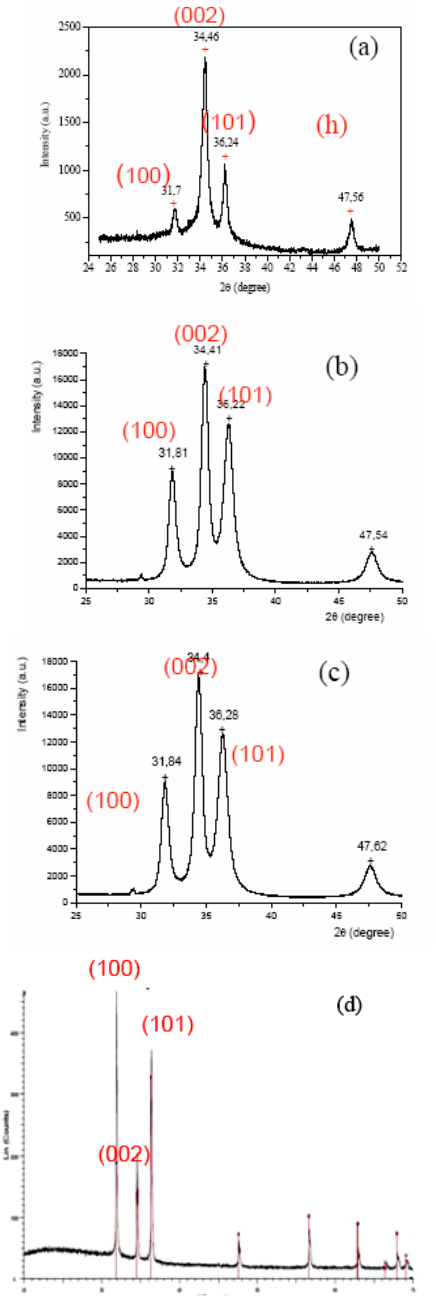


*Fig. 8. XRD patterns of ZnO 1D nanostructures grown on substrates seeded with gold thin films (a-b), preprepared ZnO nanoparticles thin film (c) and sol-gel drived ZnO thin film (d).*

These results are confirmed by the scanning electron microscopy (SEM) images presented in Fig. 7.

From the FTIR spectra of ZnO nanostructures grown on silicon substrate seeded with gold nanoparticles one can observed ZnO peaks situated at 441 and 600cm$^{-1}$ (Fig. 9). The peaks corresponding to the water molecule vibrations are also observed.

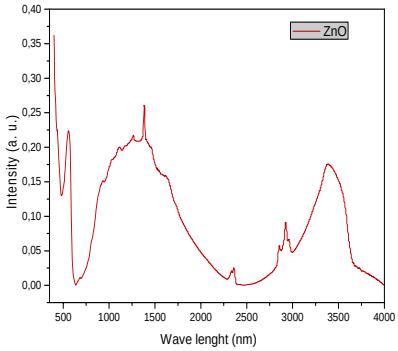


*Fig. 9. FTIR spectra of as-grown ZnO 1D nanostructures*

The temperature variation of the electrical resistivity of the as-grown nanostructures in solution at 95$^{o}$C and annealed at temperatures up to 250$^{o}$C are presented in Figure 10. These results show very good semiconductive properties, suitable for using in (opto)electronic devices.

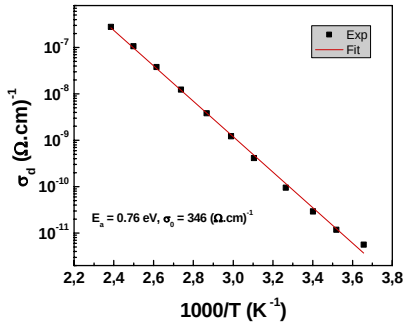


a

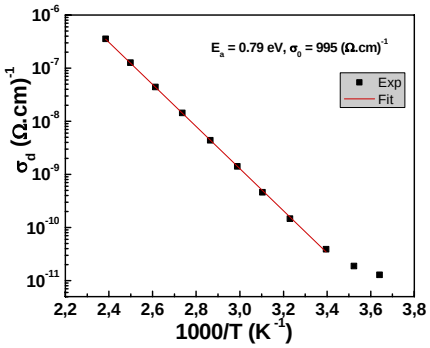


b

*Fig. 10. The variation of electrical resistivity with the temperature for the as-grown ZnO nanostructures sample (a) and the same sample after thermal annealing at 250$^{o}$C (b).*

For the sample as-grown in solution without other annealing, the σ vs 1/T curve (Fig. 10 a) suggests an extended conduction mechanism plus a delocalized phonon conduction mechanism (for the temperature range of 270-294$^{o}$C). The thermal annealing at temperatures up to 250$^{o}$C has improved the electrical properties of the semiconductive 1D nanostructures, fell three times the electrical resistivity from 995 to 346 (Ωcm)$^{-1}$, by reducing the conductivity due to the delocalized phonons (Fig. 10 b). In future studies we will develop this aspect.

## 4. Conclusions

ZnO 1D nanostructures were grown by CBD at 95$^{o}$C, using three types of thin film catalyst-seeded templates: gold thin film, dispersion of ZnO nanoparticles thin film and ZnO sol-gel drived thin film.

The effect of these three seeded thin film templates on the morphology, aspect ratio and crystalline structure of the grown 1D nanostructures were investigated. All the obtained 1D nanostructures are nanorods-like structures, with aspect ratio (length/ diameter) ranging from 6 to 10. The morphology of the seeded substrate significantly affects the crystallographic orientation, the aspect ratio length/diameter and the growing mechanism of 1D nanostrucures.

All the as-grown 1D nanostructures are well crystallized, with wurtzite-type hexagonal structure and different crystallographic orientations. Smaller size and uniform shape of seeds lead to more uniform morphology and higher degree of crystals orientations perpendicular to the substrate.

The electrical measurements on the as-grown nanostructures in solution at 95$^{o}$C show very good semiconductive properties, suitable for using in (opto)electronic devices. The thermal annealing at temperatures up to 250$^{o}$C improve the electrical properties of the semiconductive 1D nanostructures, fell three times the electrical resistivity from 995 to 346 (Ωcm)$^{-1}$, by reducing the conductivity due to the delocalized phonons.

**Aknowledgements**

This work was supported by NMT ERA-NET-MULTINANOWIRES Grant (Contract NMT 7-029-2010 and Advanced Grant Contract nº 228144).

## References

[1] L. E. Greene, M. Law, J. Goldberger, F. Kim, J. C. Johnson, Y. Zhang, R. J. Saykally, P. Yang, Chem. Int. Ed. **42**, 3031 (2003).
[2] L. Mazeina, Y. N. Picard, and S. M. Prokes, Crystal Growth & Design **9**, 1164 (2009).
[3] A. Umar, B. K.Kim, J. J. Kim, Y. B. Hahn, Nanotechnology **18,** 175606-1 (2007).
[4] C. J. Chen, W. L. Xu, and M. Y. Chern, Adv. Mater. **19**, 3012 (2007).

[5] Z. J. Li, Z. Qin, Z. H. Zhou, L. Y. Zhang, Y. F. Zhang, Nanoscale Res Lett **4,** 1434 (2009).
[6] L. Liao, H. B. Lu, J. C. Li, C. Liu, D. J. Fu, Applied Physics Letters **91**, 173110-1 (2007).
[7] B .Baruwati, K. D. Kishore, S. V. Manorama, Sensors and Actuators B Chemical **119**, 676 (2006).
[8] G. Shi, C. M. Mo, W. L. Cai, L. D. Zhang, Solid State Communications **115**, 253 (2000).
[9] E. A. Meulenkamp, J. Phys. Chem. B **102,** 5566 (1998).
[10] M. Vafaee, M. S. Ghamsari, Materials Letters **61**, 3265 (2007).
[11] S. G. Devi, V. B. Subrahmanyam, S. C. Gadkari, S. K. Gupta, Ana. Chim. Acta **568**, 41 (2006).
[12] H. Tang, M. Yan, X. Ma, H. Zhang, M. Wang, D. Yang, Sensor. Actuat. B-Chem. **113,** 324 (2006).
[13] M. K. Patra, K. Manzoor, M. Manoth, S. C. Negi, S. R. Vadera, N. Kumar, Defence Science Journal **58** 636 (2008).
[14] J. H. Shin, J. Y. Song, H. M. Park, Materials Letters **63**, 145 (2009).
[15] L. Guo, S. Yang, C. Yang, P. Yu, J. Wang, W. Ge, G. K. L. Wong, Chem. Mater. **12**, 2268 (2000).
[16] L. Guo, S. Yang, C. Yang, P. Yu, J. Wang, W. Ge, G. K. L. Wong, Appl. Phys. Lett., **76,** 2901 (2000).
[17] R. Hong, T. Pan, J. Qian, H. Li, Chemical Engineering Journal **119**, 71 (2006).
[18] S., Liufu, H. Xiao, Y. Li, Powder Technology **145**, 20 (2004).
[19] A. Dev, S, Chaudhuri, B. N. Dev, Bull. Mater. Sci. **31**, 551 (2008).

*Corresponding author: viorica.musat@ugal.ro